Philosophical Magazine Letters,
Vol. 85, No. 10, October 2005, 513–521

Taylor & Francis
Taylor & Francis Group

Effect of aspect ratio on the compressive deformation and fracture behaviour of Zr-based bulk metallic glass

Z. F. ZHANG*†, H. ZHANG†, X. F. PAN†‡, J. DAS§¶ and J. ECKERT§¶

†Shenyang National Laboratory for Materials Science, Institute of Metal Research, Chinese Academy of Sciences, 72 Wenhua Road, Shenyang 110016, China
‡School of Materials Science and Engineering, Tianjin University, Tianjin 300072, China
§Darmstadt University of Technology, Department of Materials and Geo Sciences, Physical Metallurgy Division, Petersenstr. 23, D-64287 Darmstadt, Germany
¶IFW Dresden, Institute of Metallic Materials, P.O. Box 270016 D-01171 Dresden, Germany

(*Received 8 June 2005; in final form 28 July 2005*)

The compressive deformation and fracture features of $Zr_{59}Cu_{20}Al_{10}Ni_8Ti_3$ bulk metallic glassy samples with aspect ratios in the range of 0.67–2.00 have been investigated. The compressive plastic strain of the glass monotonically increases with decreasing aspect ratio, but the maximum strength almost maintains a constant value of 1.77–1.88 GPa. All the compressive shear-band angles are equal to $\sim 40^\circ$ if modified by the rotation of the primary shear bands.

1. Introduction

Metallic glasses often display extreme mechanical properties. For example, the extremely high strength is one of the merits of metallic glasses; however, it is often accompanied by remarkably little plastic deformation at room temperature owing to catastrophic fracture [1–6]. Accordingly, the deformation and fracture mechanisms of metallic glasses are significantly different from those of crystalline materials [7]. In recent decades, the extraordinary mechanical behaviour of bulk metallic glasses (BMG) materials has attracted worldwide interest [7–18]. In general, the plastic deformation of metallic glasses is localized in narrow shear bands, followed by the rapid propagation of these shear bands and sudden fracture [1–6, 12]. A number of investigations have revealed that the shear fracture of BMGs does not occur along the maximum shear stress plane no matter whether under compressive or tensile loading [3, 10, 11, 13–20]. BMGs may exhibit a certain ductility when subjected to compressive or bending loads due to the formation of multiple shear bands [4, 5, 9, 21, 22]. This gives rise to the question how the formation and development of the shear bands control the ductility of the BMGs. Recently, Conner *et al*. [9] found that thin metallic glassy ribbons showed ductility without failure in bending, but thicker plates fail catastrophically. Another possible way to trigger the formation of multiple shear bands is to apply confining pressure to the BMG samples.

*Corresponding author. Email: zhfzhang@imr.ac.cn

Philosophical Magazine Letters
ISSN 0950–0839 print/ISSN 1362–3036 online © 2005 Taylor & Francis
http://www.tandf.co.uk/journals
DOI: 10.1080/09500830500395237

For example, Davis and Kavesh [2], Lewandowski and Lowhaphadu [10] and Lu and Ravichandran [12] have investigated the effect of hydrostatic pressure on the flow and fracture behaviour of Zr-based metallic glasses. They found that BMGs can exhibit large inelastic deformation of more than 10% under confinement. In addition, Bruck *et al*. [8] investigated the effect of two aspect ratios (1: 2 and 2:1) on the compressive properties and found a slight increase in the yield strength and obvious increase in the compressive plasticity. This indicates that the observed ductility of BMGs strongly depends on the sample geometry and the applied loading modes. In the present work, we attempt to systematically reveal the effects of aspect ratio (0.67–2.00) on yield strength, compressive plasticity as well as the corresponding shear deformation and fracture mechanisms for a $Zr_{59}Cu_{20}Al_{10}Ni_8Ti_3$ metallic glass.

2. Experimental procedures

A master ingot with composition $Zr_{59}Cu_{20}Al_{10}Ni_8Ti_3$ was prepared by arc-melting elemental Zr, Cu, Al, Ni and Ti with a purity of 99.9% or better in a Ti-gettered argon atmosphere. To ensure homogeneity, the master alloy ingot was re-melted several times and subsequently cast into a copper mold with a diameter of 3 mm. The amorphous structure of the as-cast alloy was checked by standard X-ray diffraction (Philips PW1050 diffractometer using Co Kα radiation). In the XRD pattern of the as-cast alloy, there are only broad diffraction maxima and no peaks of crystalline phase can be seen [15]. Before compression testing, the metallic glassy rod was cut into samples with different heights of 2, 3, 4, 5 and 6 mm, respectively. This yields different aspect ratios H/D of height (H) to diameter (D), i.e. 0.67, 1.00, 1.33, 1.67 and 2.00. After cutting, the two ends of all the samples were carefully polished with a mold to ensure parallelism. The compression tests were conducted at a strain rate of about $10^{-4}\,s^{-1}$ with a MTS 810 testing machine at room temperature. After compression, all the specimens were investigated with a Cambridge S360 scanning electron microscope (SEM) to reveal the fracture surface morphology and the fracture features.

3. Results and discussion

3.1. *Compressive properties*

Figure 1a shows the engineering stress–strain curves of the $Zr_{59}Cu_{20}Al_{10}Ni_8Ti_3$ glassy samples with different aspect ratios (H/D). For better visibility, the curves are shifted along the strain axis. The stress–strain curve of the BMG sample (A) with an aspect ratio of $H/D = 2.00$ is identical with the data reported for a variety of other BMG samples exhibiting also the standard aspect ration of 2.0, i.e. its compressive plasticity is smaller than 1% and the fracture stress is quite close to the yield strength of the material [10, 11, 14, 15]. With decreasing aspect ratio, the yield strength remains almost constant. However, the plastic strain prior to failure increases monotonically. For the BMG samples (B-D) with an aspect ratio range

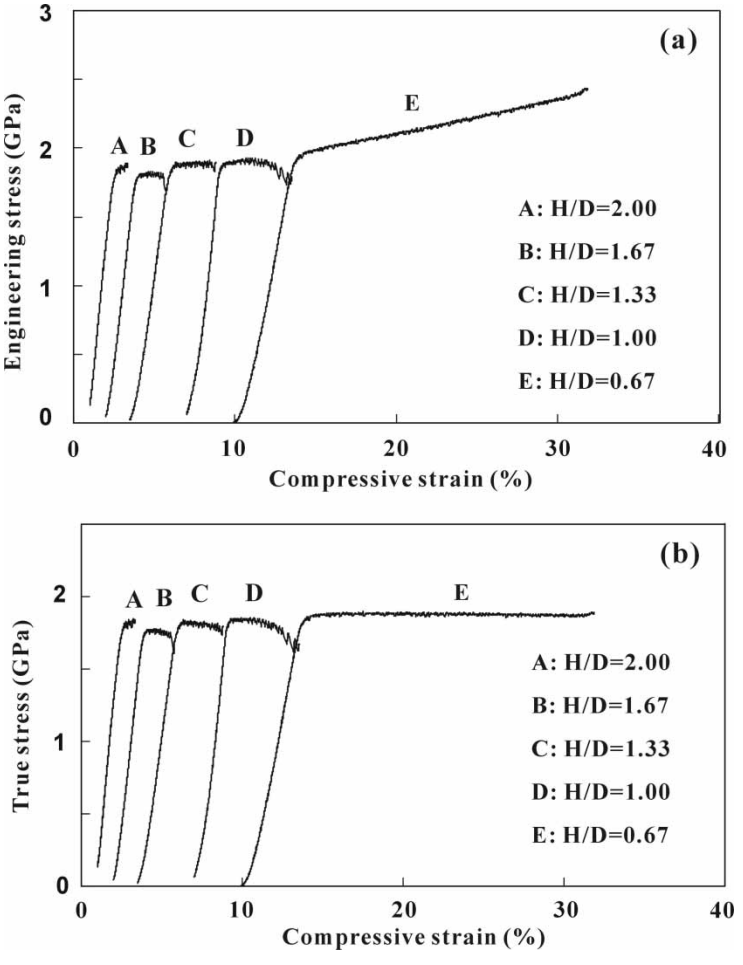

Figure 1. (a) Engineering stress–strain curves and (b) true stress–strain curves of $Zr_{59}Cu_{20}Al_{10}Ni_8Ti_3$ metallic glassy samples with different aspect ratios.

of $H/D = 1.00$–1.67, it seems that there is slight work-hardening observable in the engineering stress–strain curves. However, the flow stress of the BMG sample (E) with an aspect ratio of $H/D = 0.67$ continuously increases with increasing plastic strain from a yield strength ($\sim$1.91 GPa) to a high level (>2.50 GPa), which is indicative of work-hardening. To clarify whether there exists work-hardening behaviour or not, the true stress–strain curves of all the metallic glass samples are plotted in figure 1b. It can be clearly seen that the glassy samples do not display any work-hardening feature. The obvious increase in flow stress of the glassy sample with an aspect ratio of 0.67 can be attributed to a significant change of cross-sectional area at high strains, which is consist with the report by Bruck *et al*. [8]. However, considering the increase in the cross-section of the samples at large compressive strain, there should be no obvious work-hardening behaviour in the stress–strain curve of a Cu-based glass as reported by Das *et al*. [23].

The dependence of yield strength and plastic strain prior to failure on the aspect ratio of the Zr-based metallic glass is shown in figure 2. The yield strength of

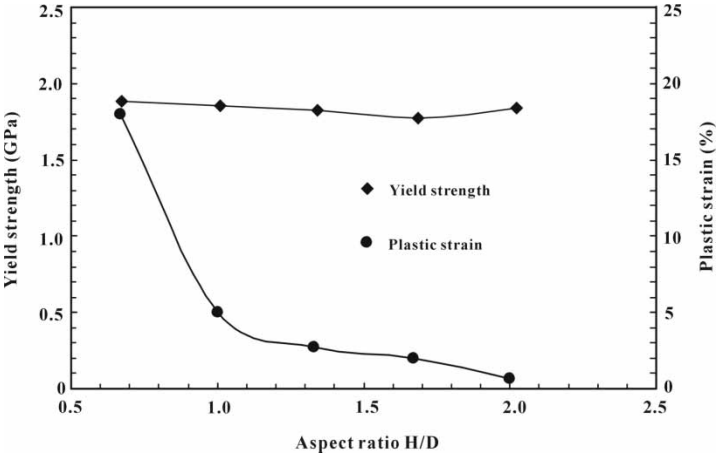

Figure 2. Dependence of yield strength and compressive plasticity on the aspect ratio of $Zr_{59}Cu_{20}Al_{10}Ni_8Ti_3$ metallic glassy samples.

all the samples is almost constant (from 1.77 to 1.88 GPa), independent of the aspect ratio. However, the compressive plasticity of the glass monotonically increases with decreasing aspect ratio. It seems that there are two sample regions, i.e. a region with low plasticity ($< 5\%$) for $H/D \geq 1.00$ and a region with high plasticity ($> 18\%$) for $H/D \leq 1.00$. This indicates that the aspect ratio plays a more important role for the plasticity than the yield strength for metallic glassy materials, especially at smaller aspect ratio.

3.2. *Deformation and fracture features*

After compression, BMG samples normally fail in a pure shear mode. The shear fracture angles of the BMG samples (A–D) with an aspect ratio range of 1.00–2.00 are smaller than 45°, as shown in figure 3a–d. This agrees well with previous observations for other BMGs [3, 10, 11, 13–16, 18–20]. Meanwhile, the shear fracture angle slightly increases from 40° to 42.5° with the aspect ratio decreasing from 2.00 to 1.00, as listed in table 1. This means that the non-standard BMG samples also fail in the same mode as the standard BMG samples with an aspect ratio of 2.00. In particular, the shear fracture behaviour of the non-standard BMG samples does not follow the Tresca criterion either, but can be well explained by the Mohr–Coulomb criterion [3, 10, 11, 13–16, 18–20].

For the glassy sample with the small aspect ratio of 0.67, it can be seen that multiple shear bands formed on the surface, as shown in figure 4a. The primary shear bands are inclined by an angle of about 46° to the loading direction. This shear-band angle is slightly higher than that of the other samples with a larger aspect ratio (see figure 3). This result is quite similar to the observations in a Ti-based nanostructure dendrite composite with a high ductility [17]. Coarse shear bands normally originated from the edge of the sample and then propagated towards the centre of the specimen, as shown in figure 4b. Some secondary shear bands were activated and interact with the primary shear bands, as shown in figure 4c and d. The interactions between primary and secondary shear bands often induce a large

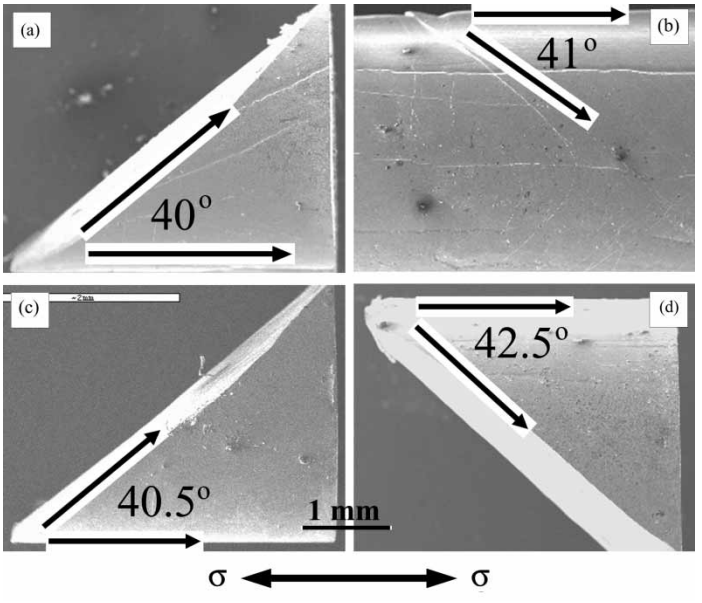

Figure 3. Compressive shear deformation and fracture of $Zr_{59}Cu_{20}Al_{10}Ni_8Ti_3$ metallic glassy samples with different aspect ratios. (a) $H/D = 2.00$; (b) $H/D = 1.67$; (c) $H/D = 1.33$; (d) $H/D = 1.00$.

Table 1. Compressive plasticity and shear-band angles of $Zr_{59}Cu_{20}Al_{10}Ni_8Ti_3$ metallic glassy samples with different aspect ratios.

Aspect ratio (H/D)	Plastic strain (ε_p, %)	Measured shear-band angle (θ_C^F, °)	Initial shear-band angle (θ_C^O, °)
2.00	0.7	40	39.8
1.67	2.0	41	40.6
1.33	2.7	40.5	40.1
1.00	5.0	42.5	40.7
0.67	18.0	46	40.6

shift from their propagation path, as indicated by the arrows in figure 4d. This suggests that the multiple shear bands and their interactions may provide a significant contribution to the high ductility of the BMG samples with small aspect ratio.

3.3. *Effects of aspect ratio on the shear deformation*

From the experimental results above, it can be concluded that the compressive plasticity and the formation of multiple shear bands are strongly affected by the aspect ratio of the BMG samples. During compression, besides the uniaxial stress σ, there is often a lateral stress σ_L induced by friction between the end of the samples and the crosshead of the testing machine [24]. For a BMG sample with a large aspect ratio, its stress distribution can be schematically illustrated as in figure 5a. The lateral stress σ_L acts only close to the end of the sample; accordingly, the shear

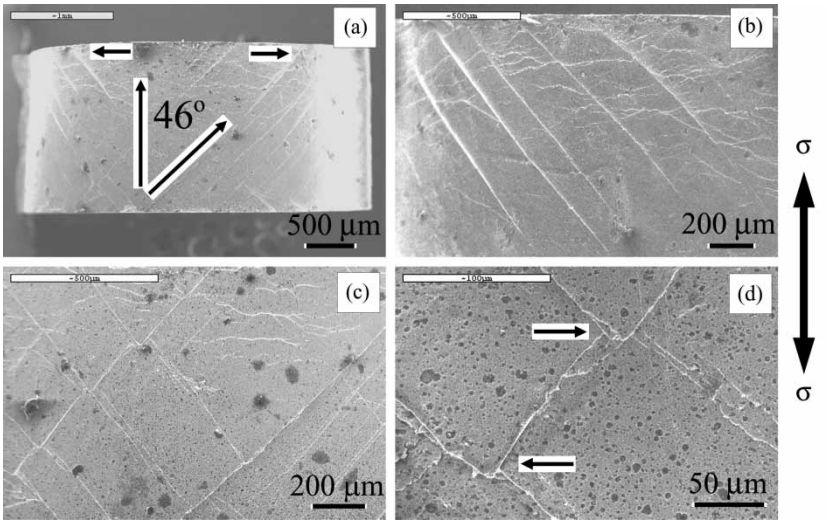

Figure 4. Compressive shear deformation patterns of a $Zr_{59}Cu_{20}Al_{10}Ni_8Ti_3$ metallic glassy sample with an aspect ratio of 0.67 observed at (a) and (b) low magnifications; (c) and (d) high magnifications.

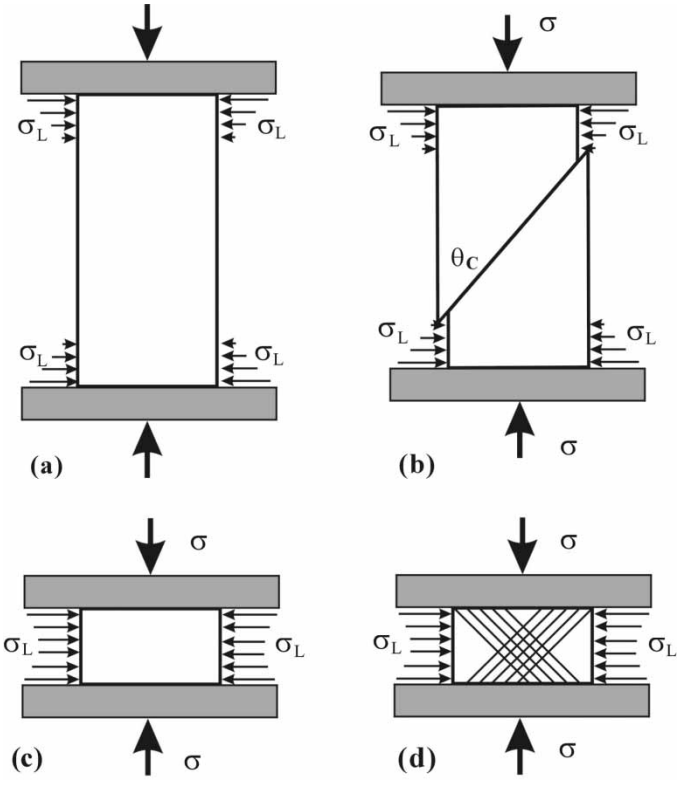

Figure 5. Schematic illustrations of (a) weak confining effect and (b) singular shear fracture under the condition at large aspect ratio; (c) strong confining effect and (d) formation of multiple shear bands under condition at small aspect ratio.

fracture process can be illustrated as in figure 5b. In this case, it is expected that the lateral stress σ_L plays only a minor role for determining the yield strength, the plastic deformability and the shear fracture of the BMG samples. Since the shear fracture angle θ_C of the BMG samples is smaller than 45° (see table 1), it is suggested that the Mohr–Coulomb criterion can well explain this fracture mechanism, i.e. the critical shear fracture condition is [3, 10, 13–15]:

$$\tau \geq \tau_0 + \mu \cdot \sigma_n, \tag{1}$$

where μ is the slope of the critical shear fracture line AB, and can be expressed as

$$\mu = c\, tg(2\theta_C). \tag{2}$$

With decreasing aspect ratio of the BMG samples, the lateral stress σ_L will continuously increase due to the strong effect of the friction between the sample and the crosshead. Therefore, the stress distribution of such BMG samples can be schematically illustrated as in figure 5c. Once the primary shear bands have formed, their rapid propagation will be difficult owing to the strong constraint imposed by the lateral stress σ_L and the cross-head of the testing machine, as illustrated in figure 5d. The constraint often causes a three-axial compressive stress on the samples and is easy to induce the formation of multiple shear bands, as schematically illustrated in figure 5d. Lu and Ravichandran [12] found that the inelastic strain is over 10% with the formation of multiple shear bands when their Zr-based glassy samples were subjected to a lateral confinement. However, work-hardening did not occur during plastic flow of the Zr-based glass under confinement. With further applying compressive stress, the density of the shear bands will increase continuously, resulting in a high compressive plasticity, as shown in figure 1. Lewandowski and Lowhaphadu [10] found for a Zr-based BMG that the shear fracture angles are independent of an applied hydrostatic pressure. In the present investigation, the lateral stress σ_L can also be regarded as hydrostatic pressure and does not change the shear fracture angle θ_C. In other words, for identical BMG samples with different aspect ratios, the formation of shear bands should follow the Mohr–Coulomb criterion with the same constant μ. Consequently, the shear band angles θ_C of all the BMG samples should be independent of the aspect ratio. However, the shear bands make a larger angle (~46°) with respect to the loading direction in the BMG sample with a smaller aspect ratio (0.67). In particular, the shear band angle is larger than 45°, which seems to be impossible when taking the Mohr–Coulomb criterion into account. In our previous work [17], the same shear fracture mode was observed for some Ti-based nanostructure composites with ductile dendrites. It was explained by a rotation mechanism of the primary shear bands due to a high compressive plasticity. In the present result, it is noted that the ductility of the BMG sample with an aspect ratio of 0.67 also reaches a very high level (~18%). Therefore, the rotation mechanism of the shear bands can be applied to the present result. In our model, a relationship among θ_C^O, θ_C^F and the plastic strain ε_P can be established by taking the rotation mechanism into account [17], i.e.

$$\sin(\theta_C^O) = \sqrt{1 - \varepsilon_P}\sin(\theta_C^F). \tag{3}$$

Here, θ_C^O is the initial shear band angle and θ_C^F is the final measured shear band angle after rotation. Thus, one can approximately estimate the initial shear band angle θ_C^O if the compressive plastic strain ε_P and the final measured shear

band angle θ_C^E are known. The calculated data are listed in table 1 for comparison. It can be seen that all the initial shear band angles θ_C° are quite close to $\sim 40^\circ$ for the BMG samples with an aspect ratio range of 0.67–2.00. This result is consistent with the previous observations for other BMG samples and follows the Mohr–Coulomb criterion [3, 10, 11, 13–16, 18–20]. It indicates that a smaller aspect ratio can impose a significant constraint on the BMG samples, leading to the formation of multiple shear bands and a high compressive plasticity, which in turn result in an obvious rotation of the initial shear bands.

4. Conclusions

The compressive ductility of a $Zr_{59}Cu_{20}Al_{10}Ni_8Ti_3$ bulk metallic glass strongly depends on the aspect ratio used for testing the samples; however, the yield strength remains almost constant. The large ductility of the metallic glassy sample with a small aspect ratio can be attributed to the formation of multiple shear bands induced by the confining pressure. The shear fracture angle is normally smaller than 45°, and slightly increases with decreasing aspect ratio due to a rotation process of the initial shear bands at a high compressive strain level.

Acknowledgements

The authors would like to thank H. Grahl and H. Schulze for sample preparation, and G. Yao, J. L. Wen, H. H. Su and W. Gao for mechanical tests and the SEM observations. This work was supported by the National Natural Science Funds of China (NSFC) under grant Nos. 50401019 and 50323009, the 'Hundred of Talents Project' by the Chinese Academy of Sciences and the EU within the framework of the RTN-network on ductile BMG composites (MRTN-CT-2003-504692). One of the authors (Z. F. Zhang) is also with the Multi-Component Amorphous and Nanocrystalline Systems (MANS) Research Team funded by the Chinese Academy of Sciences.

References

[1] A.S. Argon, Acta Metall. **27** 47 (1979).
[2] L.A. Davis and S. Kavesh, J. Mater. Sci. **10** 453 (1975).
[3] P.E. Donovan, Acta Metall. **37** 445 (1989).
[4] H.J. Leamy, H.S. Chen and T.T. Wang, Metall. Trans. **3** 699 (1972).
[5] C.A. Pampillo, J. Mater. Sci. **10** 1194 (1975).
[6] F. Spaepen, Acta Metall. **25** 407 (1977).
[7] R.W.K. Honeycombe, *Plastic Deformation of Metals* (Cambridge University Press, Cambridge, 1969).
[8] H.A. Bruck, T. Christman, A.J. Rosakis, *et al*., Scripta Metall. Mater. **30** 429 (1994).
[9] R.D. Conner, Y. Li, W.D. Nix, *et al*., Acta Mater. **52** 2429 (2004).
[10] J.J. Lewandowski and P. Lowhaphandu, Phil. Mag. **82** 3427 (2002).

[11] C.T. Liu, L. Heatherly, D.S. Easton, *et al*., Metall. Mater. Trans. **29** 1811 (1998).
[12] J. Lu and G. Ravichandran, J. Mater. Res. **18** 2039 (2003).
[13] A.C. Lund and C.A. Schuh, Intermetallics **12** 1159 (2004).
[14] W.J. Wright, R. Saha and W.D. Nix, Mater. Trans. **42** 642 (2001).
[15] Z.F. Zhang, J. Eckert and L. Schultz, Acta Mater. **51** 1167 (2003).
[16] Z.F. Zhang, G. He, J. Eckert, *et al*., Phys. Rev. Lett. **91** 045505 (2003).
[17] Z.F. Zhang, G. He, H. Zhang, *et al*., Scripta Mater. **52** 945 (2005).
[18] Z.F. Zhang and J. Eckert, Phys. Rev. Lett. **94** 094301 (2005).
[19] G. He, Z.F. Zhang, W. Löser, *et al*., Acta Mater. **51** 2383 (2003).
[20] A. Inoue and B.L. Shen, Adv. Mater. **16** 2189 (2004).
[21] H. Chen, Y. He, G.J. Schiflet, *et al*., Nature **367** 541 (1994).
[22] J. Schroers and W.L. Johnson, Phys. Rev. Lett. **93** 255506 (2004).
[23] J. Das, M.B. Tang, K.B. Kim, *et al*., Phys. Rev. Lett. **94** 205501 (2005).
[24] Z.F. Zhang, D. Brunner, C. Scheu, *et al*., Z. Metalld. **96** 62 (2005).